Resolving Point Defects in the Hydration Structure of Calcite (10.4) with Three-Dimensional Atomic Force Microscopy

Hagen Söngen,[1,2,*] Bernhard Reischl,[3,†] Kazuki Miyata,[4] Ralf Bechstein,[1] Paolo Raiteri,[3,5]
Andrew L. Rohl,[3] Julian D. Gale,[3,5] Takeshi Fukuma,[4,6] and Angelika Kühnle[1,7,‡]

[1]*Institute of Physical Chemistry, Johannes Gutenberg University Mainz, Duesbergweg 10-14, 55099 Mainz, Germany*
[2]*Graduate School Materials Science in Mainz, Staudinger Weg 9, 55128 Mainz, Germany*
[3]*Curtin Institute for Computation and Department of Chemistry, Curtin University,*
P.O. Box U1987, Perth, Western Australia 6845, Australia
[4]*Division of Electrical Engineering and Computer Science, Kanazawa University, Kanazawa 920-1192, Japan*
[5]*The Institute for Geoscience Research (TIGeR), Curtin University, P.O. Box U1987, Perth, Western Australia 6845, Australia*
[6]*WPI Nano Life Science Institute (WPI-NanoLSI), Kanazawa University, Kanazawa 920-1192, Japan*
[7]*Physical Chemistry I, Bielefeld University, Universitätsstraße 25, 33615 Bielefeld, Germany*

It seems natural to assume that defects at mineral surfaces critically influence interfacial processes such as the dissolution and growth of minerals in water. The experimental verification of this claim, however, is challenging and requires real-space methods with utmost spatial resolution, such as atomic force microscopy (AFM). While defects at mineral-water interfaces have been resolved in 2D AFM images before, the perturbation of the surrounding hydration structure has not yet been analyzed experimentally. In this Letter, we demonstrate that point defects on the most stable and naturally abundant calcite (10.4) surface can be resolved using high-resolution 3D AFM—even within the fifth hydration layer. Our analysis of the hydration structure surrounding the point defect shows a perturbation of the hydration with a lateral extent of approximately one unit cell. These experimental results are corroborated by molecular dynamics simulations.

Defects have been suggested as the nucleus for dissolution and growth processes on the calcite (10.4) surface [1,2]. Experimentally, Harstad and Stipp [2] have reported that even trace amounts of impurities present in natural calcite samples (such as Mg, Fe, Sr, Mn) influence the dissolution. Moreover, in a recent theoretical study, the substitution of Ca ions with similar divalent ions on the calcite (10.4) surface has been found to significantly alter the affinity of water towards the surface [3]. As a consequence, trace amounts of defects can steer the competitive adsorption between water and organic molecules—a highly relevant interplay in the field of biomineralization [3].

Water at surface defects on calcite (10.4) has been theoretically studied using density functional theory by Lardge *et al.* [4]. The simulation system included the calcite surface with a carbonate vacancy, a calcium vacancy, and a single water molecule. Compared to the flat (10.4) terrace, the binding energy of water at both defects has been found to increase (by 0.56 and 0.66 eV for the carbonate and calcium vacancy, respectively). Moreover, the water molecule was found to dissociate at carbonate vacancies, but not at calcium vacancies.

A recent molecular dynamics (MD) study by Reischl *et al.* [5] has considered bulk water instead of a single water molecule as well as the presence of a nanoscopic atomic force microscopy (AFM) tip. The authors have simulated both calcium and carbonate vacancies as well as the substitution of a single Ca atom with a Mg atom. Two major results have been obtained [5]. First, the defects were found to be stable over the time scale of the simulations—even though the vacancies carried a local charge of $\pm 2e$. This behavior has been observed in the presence and in the absence of the AFM tip.

Second, at the calcium vacancy, the surrounding water structure has been found to be significantly perturbed, while at the carbonate vacancy, the distortion of the water structure was less pronounced. In the case of the magnesium substitution, water has been found to be shifted closer to the surface (similar to the Mg ions on the dolomite surface presented in Ref. [6]). Therefore, in all cases, defects influence the water structure in their vicinity. For the three different types of defects that have been considered, the lateral extent of the influence on the hydration structure has been reported to be on the order of 2×2 surface unit cells.

On the basis of these purely theoretical results, the authors raised the question of whether the predicted changes at the defect sites can be resolved by AFM. So far, surface defects at the calcite-water interface have only been observed in 2D AFM experiments [7,8]. In these studies, the observation of defects has been used to characterize the AFM tip—only atomically sharp AFM

tips image single atomic-scale features, such as point defects. However, the defect itself and its hydration structure have not been the focus of these studies. In this Letter, we present high-resolution 3D AFM experiments to assess the hydration structure in the vicinity of point defects at the calcite-water interface, which we compare to atomistic simulations of calcite surfaces with point defects and AFM simulations with a model silica tip. We show that the defect detectably perturbs the hydration structure up until even the fifth hydration layer. Therefore, we are able to answer the above question in the affirmative; with 3D AFM defects can, indeed, be resolved by their perturbation of the surrounding hydration structure.

Experiments were performed with a custom-built AFM [9,10] using the 3D mapping technique, where the position of the oscillating AFM tip is additionally modulated vertically [11]. Silicon cantilevers (AC55, Olympus) with a nominal spring constant of 85 N m^{-1} and an eigenfrequency ν_e of approximately 1.2 MHz in water were used. In most cases, the cantilevers were coated by an additional layer of silicon (of approximately 15 nm thickness) by sputtering as described in Ref. [12]. The excitation of the cantilever was performed with a photothermal excitation system [13,14]. Amplitude and phase shift of the cantilever oscillation were detected by a commercial oscillation controller (OC4, Specs). The oscillation controller was operated in the frequency modulation (FM) mode, meaning that two feedback loops are employed to keep amplitude and phase shift constant by adjusting the excitation force amplitude and the excitation frequency ν_{exc}, respectively. The typical resolution of 3D data sets was 64×64 pixels laterally and 512 pixels vertically, with a data acquisition time on the order of 2 min. According to the solvent tip approximation [15,16], maxima in the excitation frequency shift $\nu_{exc} - \nu_e$ are interpreted as maxima in the water density (as in Ref. [6]). The crystallographic directions of the crystal were determined from the birefringence [17].

Figure 1(a) shows an atomically resolved excitation frequency shift $\nu_{exc} - \nu_e$ image of the (10.4) surface of calcite. At various positions in the image, deviations from the periodic lattice of the calcite (10.4) surface can be observed. In previous AFM works, similar atomic-scale inhomogeneities on the calcite surface have been assigned to point defects [7,8,18]. The measurements show that point defects on the surface of calcite (10.4) are present in the sample. They can be observed with the experimental setup, which also means that an atomically sharp tip has been used in this experiment.

Next, we assess whether the defects are located at fixed positions or whether they are diffusing, appearing or disappearing over the course of time. To this end, we recorded consecutive 2D images at a fixed surface site. An image recorded 2 min after the image shown in Fig. 1(a) is shown in Fig. 1(b) [19]. Several point defects are located at fixed positions (e.g., the two defects marked by the red
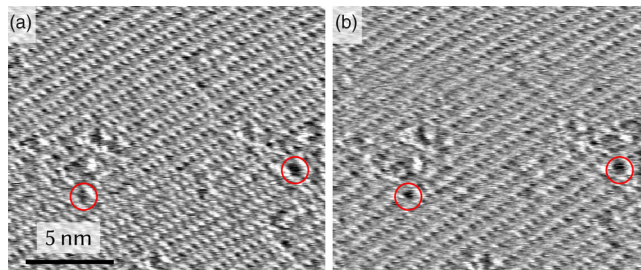

FIG. 1. AFM images of the atomically resolved calcite (10.4) surface with defects. Panels (a) and (b) show two AFM images at the same sample position recorded with a time difference of 2 min. Two red circles shown at equivalent positions in both images serve as a guide to the eye by showing the same defects, illustrating that the locations of the defects are fixed. The data range in both images is 1–6 kHz. All images are trace-down images, the $[42\bar{1}]$ direction points to the lower right corner.

circles at identical positions in both images). Observing the same deviation from the otherwise periodic calcite surface structure in consecutive images makes it highly unlikely that the deviation is an imaging artifact and, thus, confirms our assignment as a defect. Our observation is consistent with the MD simulations by Reischl *et al.* [5], which indicate that calcium and carbonate vacancies, as well as magnesium substitutions, on calcite (10.4) are stable, even in the presence of an AFM tip. Moreover, the presented data show that defects can be observed at least within a time that is similar to that taken to record a typical 3D dataset (which is on the order of 2 min).

Next, we performed 3D AFM mapping to resolve the local hydration structure surrounding a defect. Lateral slices of a 3D excitation frequency dataset extracted at different z piezodisplacements (corresponding to the different hydration layers) are presented in Fig. 2. Note that we show unfiltered experimental raw data. The surface unit cell (rectangular overlay at the bottom right in Fig. 2) of calcite (10.4) can be identified by the pattern of minima and maxima. An inhomogeneity is visible in the center of the lateral slices (indicated by the arrow in layer 1). The deviation from the otherwise periodic structure was repeatedly observed in at least three scan lines. In contrast to randomly appearing imaging artifacts such as noise, we expect this stability from a defect at a fixed surface site. By analogy to the 2D images, we interpret this inhomogeneity as a point defect. The defect does not cause a major disruption of the hydration structure. A slightly enhanced contrast (smaller or larger excitation frequency compared to equivalent sites) is visible at the defect site—even within the fifth hydration layer. Note that the defect appears at different positions within the various layers (as can be seen by using the unit cell marking as a fixed reference). In the presented data, the deviation from the otherwise periodic pattern is visible only within an area that measures one $CaCO_3$ unit, i.e., half a calcite (10.4) surface unit cell. Considering the different noise present in the experimental
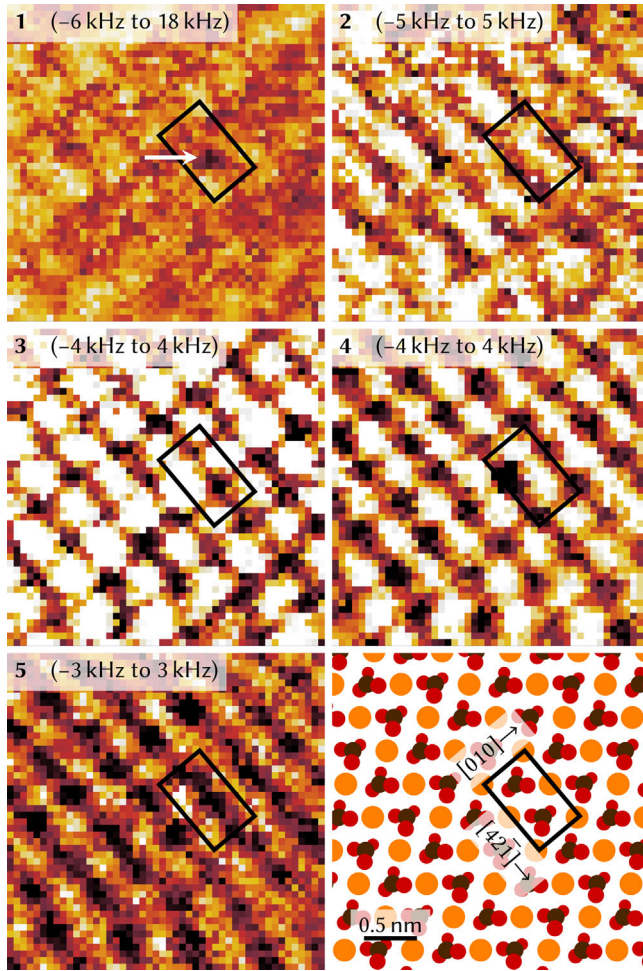
FIG. 2.   Lateral slices of a 3D excitation frequency shift dataset showing a defect. The number in each panel indicates the hydration layer, in which the lateral slice was extracted (the corresponding z piezodisplacement is shown in Fig. 3). The color scale ranges from black (low) over orange to white (high). The lower right panel shows the atomic structure of the (10.4) surface unit cell along with a scale bar that applies to all panels.
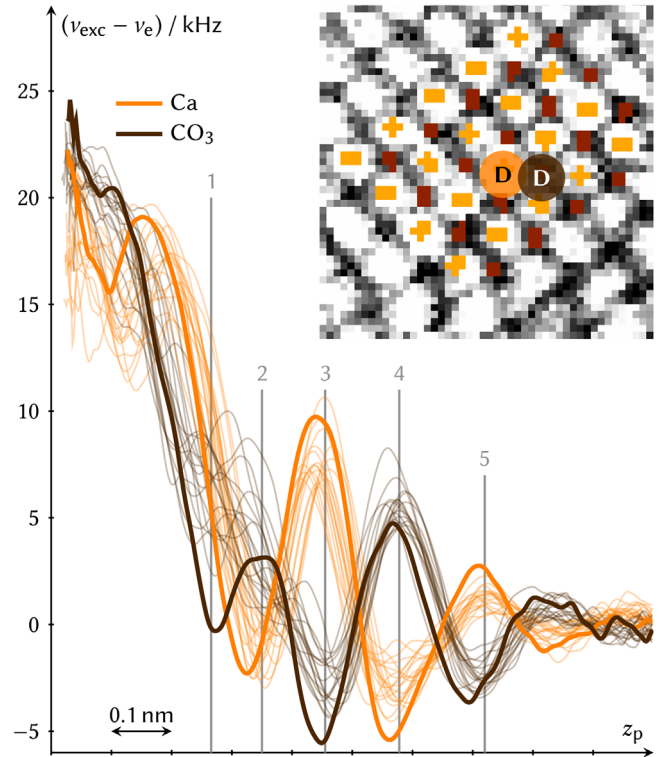

FIG. 3.   Excitation frequency shift profiles extracted above calcium ions (yellow) and carbonate groups (brown) at different sites. The extraction sites are shown in the inset. Profiles extracted at the defect site (marked with "D" in the inset) are drawn as thick lines; all other profiles are drawn as thin lines. The vertical lines (with numbers 1–5) indicate the tip-sample distance, at which the slices presented in Fig. 2 were extracted.

data and in the MD simulation data, the lateral extent fits remarkably well with the MD simulation results [5].

In Fig. 3, we compare profiles of the excitation frequency (as a function of the z piezodisplacement) obtained above defect and nondefective sites. Similar to previous works [6,20], we assign profiles with a minimum in the first layer (brown curve) to a carbonate site, the other set of curves (yellow) to Ca sites [21]. The profiles shown in Fig. 3 are drawn using thin lines for the nondefective sites and with thick lines at the defect site (indicated by the arrow in Fig. 2). The extraction sites are marked in the third layer (inset of Fig. 3) by the yellow and brown circles, while the defect sites are additionally marked with "D." To account for the finite size of the individual sites that are imaged, the profiles are averages over several pixels as indicated by the shaded area around each site in the overlay. Given the small number of equivalent surface sites considered, we show all

profiles as individual curves. The curves extracted above the defect sites (drawn with thick lines) exhibit some minor, yet systematic, differences compared to the nondefective sites (drawn using thin lines): The profile corresponding to the Ca defect site (yellow thick line) consistently exhibits the largest local maxima and the smallest local minima in the fifth, fourth and (with one exception) the third layer. This corresponds to the enhanced contrast visible at the defect site in Fig. 2. Moreover, in the first and second layer, the defect profile extracted above the Ca site is shifted closer to the surface compared to the other Ca profiles. The other defect profile (corresponding to a carbonate site, thick brown line) shows a local minimum in the first layer that is more pronounced compared to the nondefective profiles. Thus, the experimental data show that point defects, indeed, cause a minute, yet detectable, change in the hydration structure above calcite.

The magnitude of these perturbations is in good agreement with predictions from previous atomistic simulations of calcite surfaces with Ca and CO_3 vacancies and Mg^{2+} (or Fe^{2+}) substitutions [5] and additional simulations of two charge-neutral defects performed in this work, using the same methodology: a substitution of Ca^{2+} with Sr^{2+},
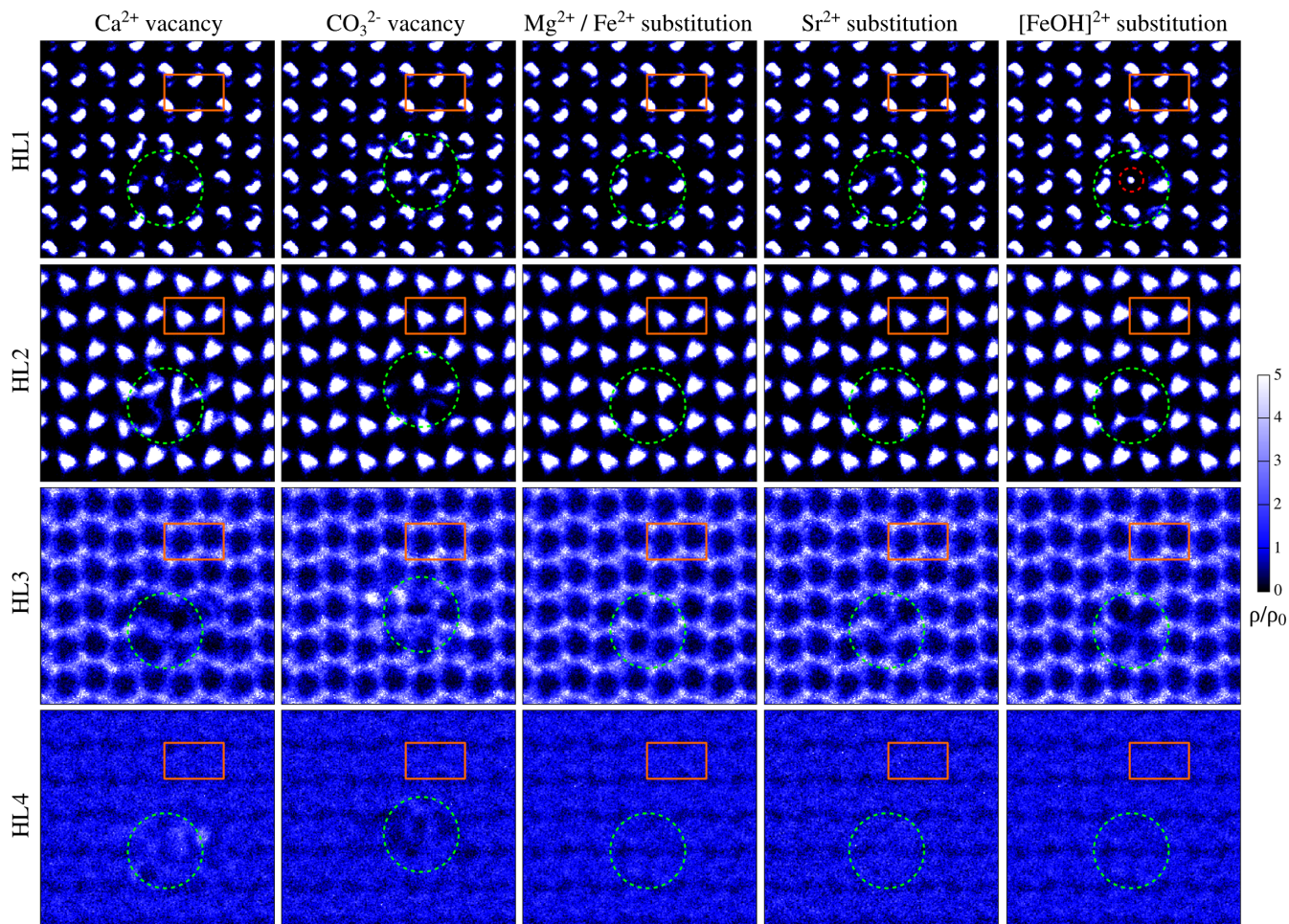
FIG. 4. Defect-induced perturbation of the calcite hydration layer structure from simulation. Lateral slices through the time averaged water oxygen density at heights corresponding to the first to fourth hydration layers (HL1–HL4) over surfaces with Ca^{2+} and CO_3^{2-} vacancies as well as Mg^{2+}/Fe^{2+}, Sr^{2+}, and $[FeOH]^{2+}$ substitutions. A calcite surface unit cell defined by the calcium ions is indicated by the orange rectangle. The position of the defect is at the center of the dashed green circles. The oxygen density peak originating from the hydroxide ion in HL1 over the Fe(III) ion is indicated by a dashed red circle. The $[42\bar{1}]$ direction points to the right, the $[010]$ direction points up.

and with Fe^{3+}, charge compensated by a OH^- ion from solution. Details regarding the simulations are described in the first section of the Supplemental Material and Fig. S1 [22]. The water density in the first four hydration layers over the five defect types is shown in Fig. 4. All defects considered are stable on the time scale of the simulation. One or two water molecules typically occupy the vacancies at any given time, with exchanges taking place on a nanosecond time scale and the hydration layer structure above the surface is more strongly perturbed compared to the charge neutral substitutions. Over the Mg^{2+}/Fe^{2+} substitution, the water molecule is at a lower position compared to Ca^{2+} in the perfect surface, whereas over Sr^{2+} the water molecule is higher, which is in good agreement with the radii of the first solvation shell of Ca, Sr, and Mg ions in solution [27]. For the $[FeOH]^{2+}$ substitution, the hydroxide oxygen atom is at a similar lateral position as the water oxygen over Ca in the perfect surface, but at a lower

height. While we are not able to identify the defects seen in experiment directly from comparison with simulation, the lateral extent of the perturbation in the hydration structure is very similar. Moreover, AFM simulations with a model silica tip, on the five defect types considered, confirm that there is a strong correlation between the changes in equilibrium hydration structure above the defect, and the force acting on the AFM tip. This is shown in detail in the Supplemental Material, Figs. S2 and S3 as vertical and lateral slices and in Fig. S4 as profiles [22]. Further, we compare the solvent tip approximation with the force curves obtained by explicitly considering the tip in the simulations in the second section of the Supplemental Material and in Fig. S5 [22].

In summary, we investigated the hydration structure above point defects at the calcite-water interface. High-resolution 3D AFM maps show that the hydration structure near point defects is perturbed—both vertically as well as

laterally. Vertically, the perturbation of the hydration structure due to the point defect is visible even in the fifth hydration layer. The lateral extent of the perturbation is on the order of a single unit cell. Both findings are in good agreement with MD simulations. To the best of our knowledge, this is the first experimental observation of the hydration structure in the vicinity of point defects with high-resolution 3D AFM in liquids. The ability to even resolve the hydration of point defects is an important milestone in the rapidly growing field of hydration layer mapping.

[*]hagen.soengen@uni-bielefeld.de
Present address: Physical Chemistry I, Bielefeld University, Universitätsstraße 25, 33615 Bielefeld, Germany.
[†]Present address: Institute for Atmospheric and Earth System Research/Physics, Faculty of Science, P.O. Box 64, University of Helsinki, 00014 Helsinki, Finland.
[‡]angelika.kuehnle@uni-bielefeld.de

[1] A. S. Lea, J. E. Amonette, D. R. Baer, Y. Liang, and N. G. Colton, Geochim. Cosmochim. Acta **65**, 369 (2001).
[2] A. O. Harstad and S. L. S. Stipp, Geochim. Cosmochim. Acta **71**, 56 (2007).
[3] M. P. Andersson, K. Dideriksen, H. Sakuma, and S. L. S. Stipp, Sci. Rep. **6**, 28854 (2016).
[4] J. S. Lardge, D. M. Duffy, M. J. Gillan, and M. Watkins, J. Phys. Chem. C **114**, 2664 (2010).
[5] B. Reischl, P. Raiteri, J. D. Gale, and A. L. Rohl, Phys. Rev. Lett. **117**, 226101 (2016).
[6] H. Söngen, C. Marutschke, P. Spijker, E. Holmgren, I. Hermes, R. Bechstein, S. Klassen, J. Tracey, A. S. Foster, and A. Kühnle, Langmuir **33**, 125 (2017).
[7] F. Ohnesorge and G. Binnig, Science **260**, 1451 (1993).
[8] S. Rode, N. Oyabu, K. Kobayashi, H. Yamada, and A. Kühnle, Langmuir **25**, 2850 (2009).
[9] T. Fukuma, M. Kimura, K. Kobayashi, K. Matsushige, and H. Yamada, Rev. Sci. Instrum. **76**, 053704 (2005).
[10] T. Fukuma and S. P. Jarvis, Rev. Sci. Instrum. **77**, 043701 (2006).
[11] T. Fukuma, Y. Ueda, S. Yoshioka, and H. Asakawa, Phys. Rev. Lett. **104**, 016101 (2010).
[12] S. M. R. Akrami, H. Nakayachi, T. Watanabe-Nakayama, H. Asakawa, and T. Fukuma, Nanotechnology **25**, 455701 (2014).
[13] T. Fukuma, Rev. Sci. Instrum. **80**, 023707 (2009).
[14] T. Fukuma, K. Onishi, N. Kobayashi, A. Matsuki, and H. Asakawa, Nanotechnology **23**, 135706 (2012).
[15] M. Watkins and B. Reischl, J. Chem. Phys. **138**, 154703 (2013).
[16] K.-i. Amano, K. Suzuki, T. Fukuma, O. Takahashi, and H. Onishi, J. Chem. Phys. **139**, 224710 (2013).
[17] S. Kuhn, M. Kittelmann, Y. Sugimoto, M. Abe, A. Kühnle, and P. Rahe, Phys. Rev. B **90**, 195405 (2014).
[18] P. Rahe, J. Schütte, and A. Kühnle, J. Phys. Condens. Matter **24**, 084006 (2012).
[19] Care was taken to select a series of images that showed a stable (nondissolving) terrace of the calcite surface without step edges. As AFM measurements are typically subject to (nonlinear) drift as well as piezocreep effects, two consecutive images do not necessarily show the exact same section of the sample surface. To align the images, the two-dimensional cross-correlation of two images was computed for each consecutive image pair. Consequently, each image was shifted by an offset given by the maximum of the cross-correlation function.
[20] T. Fukuma, B. Reischl, N. Kobayashi, P. Spijker, F. F. Canova, K. Miyazawa, and A. S. Foster, Phys. Rev. B **92**, 155412 (2015).
[21] The identification of carbonate and calcium ions is based on identifying the first hydration layer and, further, relies on interpreting the data as the water density (see Ref. [20]). As it can be difficult to ensure that the first observed layer in the 3D AFM data corresponds to the first hydration layer, the assignment might be incorrect. Importantly, this would not affect the general interpretation and conclusion of this Letter.
[22] See Supplemental Material at http://link.aps.org/supplemental/10.1103/PhysRevLett.120.116101 for details on the MD simulations and additional data regarding the simulated tip-sample force, which includes Refs. [5,12,15, 20,23–30].
[23] B. Reischl, M. Watkins, and A. S. Foster, J. Chem. Theory Comput. **9**, 600 (2013).
[24] S. Plimpton, J. Comput. Phys. **117**, 1 (1995).
[25] G. A. Tribello, M. Bonomi, D. Branduardi, C. Camilloni, and G. Bussi, Comput. Phys. Commun. **185**, 604 (2014).
[26] Y. Wu, H. L. Tepper, and G. A. Voth, J. Chem. Phys. **124**, 024503 (2006).
[27] P. Raiteri, R. Demichelis, and J. D. Gale, J. Phys. Chem. C **119**, 24447 (2015).
[28] R. T. Cygan, J.-J. Liang, and A. G. Kalinichev, J. Phys. Chem. B **108**, 1255 (2004).
[29] G. M. Torrie and J. P. Valleau, Chem. Phys. Lett. **28**, 578 (1974).
[30] A. Grossfield, WHAM: The weighted histogram analysis method, Version 2.0.9, Grossfield Laboratory, 2013, http://membrane.urmc.rochester.edu/content/wham.